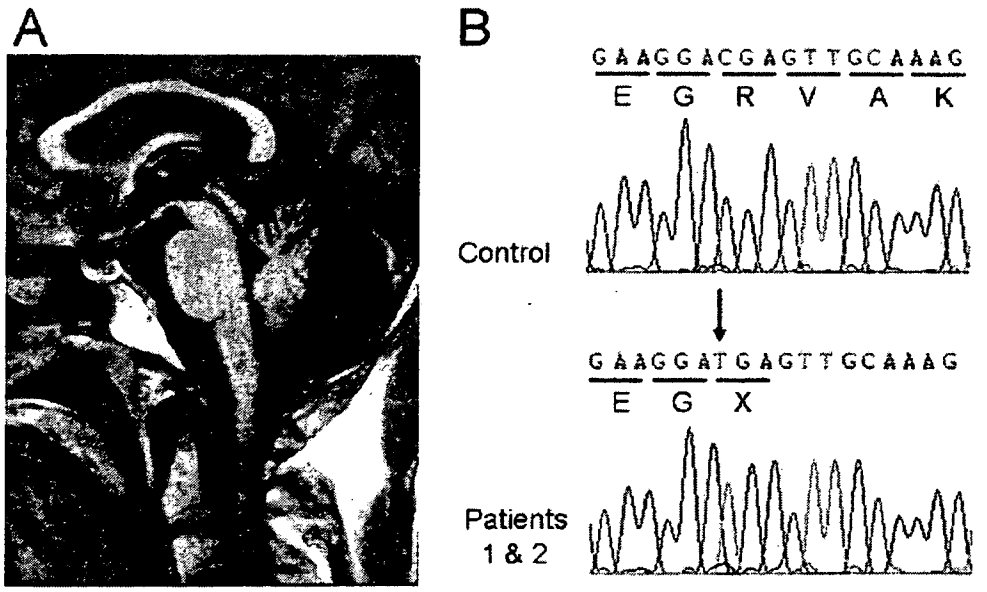

FIG. 1. Brain MRI of Patient 1 and electrogram of mutation in Patients 1 and 2. A: T1-weighted MR image of Patient 1 showing cerebellar atrophy with mega cisterna magna and cervical cord atrophy. B: The arrow indicates a homozygous C → T transition at position 6355 in exon 9 that results in a stop codon at amino acid residue 2119 (Arg2119X).

Masatoyo Nishizawa, MD, PhD*
Department of Neurology
Brain Research Institute, Niigata University
Niigata, Japan
**E-mail: nishi@bri.niigata-u.ac.jp*

References

1. Bouchard JP, Richter A, Mathieu J, et al. Autosomal recessive spastic ataxia of Charlevoix-Saguenay. Neuromuscul Disord 1998; 8:474–479.
2. Gomez GM. ARSACS goes global. Neurology 2004;62: 10–11.
3. Engert JC, Berube P, Mercier J, et al. ARSACS, a spastic ataxia common in northern Quebec, is caused by mutations in a new gene encoding an 11.5-kb ORF. Nat Genet 2000;24:120–125.
4. Shimazaki H, Takiyama Y, Sakoe K, et al. A phenotype without spasticity in sacsin-related ataxia. Neurology 2005;64:2129–2131.
5. Ouyang Y, Takiyama Y, Sakoe K, et al. Sacsin-related ataxia (ARSACS): expanding the genotype upstream from the gigantic exon. Neurology 2006;66:1103–1104.

Botulinum Toxin Treatment for Blepharospasm Associated with Myasthenia Gravis

Blepharospasm is an involuntary spasmodic contraction of the orbicularis oculi muscles, sometimes in combination with orofacial dystonia or generalized dystonia.[1] It is clinically distinguished from most cases of myasthenia gravis (MG), in which eye closure is due to fatigable weakness in the levator palpebrae muscles. In spite of these archetypal distinctions, several patients exhibiting both blepharospasm and MG have been reported.[2–7] Here, we report a patient with MG who developed facial dystonic spasms after receiving treatment for MG and showed improvements of these symptoms by botulinum toxin injection.

CASE REPORT

A 41-year-old woman came to our hospital with a 9-month history of bilateral ptosis that worsened at the end of each day. She had been using a computer more than 6-hour a day at the office. Neurological examination revealed blepharoptosis without diplopia. Repetitive nerve stimulation showed no decremental response in orbicularis oculi muscles, and no anti-AChR and anti-MuSK antibodies were detected, but the edrophonium (anticholinesterase) test was positive. A computed tomography (CT) scan of her thorax showed no thymoma. Although her ptosis improved with pyridostigmine treatment (180 mg/day), she had frequent forced eyelid closure and blinking with photophobia. The frequent blinking was improved after the cessation of the pyridostigmine

Published online 7 May 2007 in Wiley InterScience (www.interscience.wiley.com). DOI: 10.1002/mds.21558

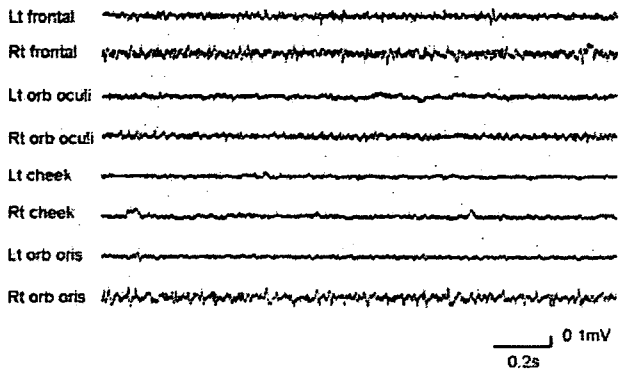

FIG. 1. Surface electromyography showing sustained contractions predominant on right side in face muscles.

treatment. However, fatigable ptosis and muscle weakness in her neck and four limbs became evident. The quantitative MG score was 10/39 points. A pulmonary function test showed normal results. On the basis of positive result of edrophonium test and fluctuation of ptosis and muscle weakness in her limbs, we diagnosed her as having generalized MG. After thymectomy and treatment with oral prednisolone (maximum dose of 80 mg on alternate days), her ptosis and muscle weakness in the limbs gradually improved. However, her frequent blinking and blepharospasm recurred in September 2005 in spite of resolution of muscle weakness in her limbs. We chose botulinum toxin treatment because MG abated. Periocular injections of 30 units of botulinum toxin (Botox, Allergan, Irvine, CA) were given after obtaining informed consent, and her blepharospasm markedly ameliorated with no exacerbation of the ptosis. Since then, she has been receiving botulinum toxin treatment every 3 months, and her fatigability has subsided. In November of 2006, however, she developed bilateral facial dystonic spasms predominantly on the right side. Surface electromyography recorded from her facial muscles showed sustained contractions of the frontal muscles, orbicularis oculi, and orbicularis oris (Fig. 1). These facial dystonic spasms were also improved by botulinum toxin treatment.

Patients with ocular MG occasionally show blepharospasm and facial spasm.[2–7] In some patients, blepharospasm itself improves with the treatment of MG using pyridstigmine, prednisolone, immunosuppressants, or thymectomy.[2–7] These reports suggest a strong association between blepharospasm and MG. One hypothesis explaining the mechanism of the coexistence of blepharospasm and MG is that myasthenic ocular muscle weakness produces abnormal feedback to the central nervous system (CNS) in patients with blepharospasm and MG.[4] Abnormalities in peripheral afferent inputs such as continual ptosis and eye blinking may interfere with motor program execution. Another hypothesis is that eye blinking compensates for eye position errors resulting from a fatigued extraocular muscle.[4] Frequent compensatory blinking may produce more abnormal feedback to the CNS. However, most patients with MG show no blepharospasm, suggesting that other environmental factors or a genetic predisposition modulates the development of blepharospasm in patients with MG. Because botulinum toxin acts by inhibiting acetylcholine release at presynaptic cholinergic junctions, it is generally contraindicated in patients with MG. Some patients with MG who presented with chronic isolated blinking had a complete ptosis lasting for 4 months by botulinum toxin injections.[5] One of the reasons the patient in this report may have shown no exacerbation of ptosis after the botulinum toxin treatment is that she received adequate treatment for MG before receiving the botulinum toxin treatment. If botulinum toxin is used in patients with blepharospasm and MG, optimized treatment of the underlying MG should precede the consideration of botulinum use.

Kenju Hara, MD, PhD
Akiko Matsuda, MD
Yuko Kitsukawa, MD
Keiko Tanaka, MD, PhD
Masatoyo Nishizawa, MD, PhD*
Department of Neurology
Brain Research Institute
Niigata University
Japan
**E-mail: nishi@bri.niigata-u.ac.jp*

Asako Tagawa, MD, PhD
Department of Immunology
National Institute of Neuroscience
NCNP
Japan

References

1. Hallet M, Daroff RB. Blepharospasm: report of a workshop. Neurology 1996;46:1213–1218.
2. Jankovic J, Ford J. Blepharospasm and orofacial-cervical dystonia: clinical and pharmacological findings in 100 patients. Ann Neurol 1983;13:402–411.
3. Jankovic J, Patten BM. Blepharospasm and autoimmune diseases. Mov Disord 1987;2:159–163.
4. Kurlan R, Jankovic J, Rubin A, Patten B, Griggs R, Shoulson I. Coexistent Meige's syndrome and myasthenia gravis. A relationship between blinking and extraocular muscle fatigue? Arch Neurol 1987;44:1057–1060.
5. Roberts ME, Steiger MJ, Hart IK. Presentation of myasthenia gravis mimicking blepharospasm. Neurology 2002;58:150-151.
6. Tsuda H, Kamei S, Mizutani T, Saito N, Ishikawa H, Omori K. Blepharospasm in a patient with thymoma and positive anti-acetylcholine receptor antibody. Rinsho Shinkeigaku 2003;43:500-502 (Japanese).
7. Kamada M, Fukutake T, Hiroyoshi Y, Sato S, Shibayama H, Nishino H. A case of myasthenia gravis associated with blepharoptosis mimicking blepharospasm. Rinsho Shinkeigaku 2004;44:54 (Japanese).

Neuropathology 2007; **27**, 121–126 doi:10.1111/j.1440-1789.2007.00754.x

Original Article

Morphometric and topographical studies of small neurons in sporadic amyotrophic lateral sclerosis spinal gray matter

Shintaro Hayashi,[1] Masakuni Amari,[2] Masamitsu Takatama[2] and Koichi Okamoto[1]

[1]Department of Neurology, Gunma University, Graduate School of Medicine and [2]Department of Neurology, Geriatrics Research Institute and Hospital, Gunma, Japan

Little attention has been paid to the degeneration of small neurons in ALS spinal gray matter. The purpose of the present paper was to undertake morphometric and quantitative analysis of the spinal gray matter of 15 ALS patients and compare findings to those of five controls. A significant reduction of small neurons in the anteromedial and intermediate parts of the gray matter were detected in ALS spinal cords with diffuse myelin pallor in the ventral aspects of the anterolateral columns outside the corticospinal tracts, and the number of small neurons in these areas was decreased significantly depending on the intensity of the myelin pallor. There were no significant alterations in the number of small neurons in the corresponding areas of ALS spinal cords without diffuse myelin pallor or in those of controls. In the posterior parts of the gray matter, there were no significant differences in the number of small neurons among ALS patients and controls. These findings strongly suggest that diffuse myelin pallor in the ventral aspects of anterolateral columns in ALS spinal cords is derived from the degeneration of small neurons in the anteromedial and intermediate parts of the gray matter.

Key words: amyotrophic lateral sclerosis, morphometry, myelin, pathology, spinal cord.

INTRODUCTION

In both sporadic and familial ALS spinal cords, the loss of large anterior horn cells is a major pathological feature. Several studies have documented that small neurons were also involved in ALS spinal gray matter.[1–5] However, their interpretations concerning the degeneration of small neurons remain controversial.[6] Tsukagoshi *et al.* and Oyanagi *et al.* indicated that involvement of small neurons might depend upon the duration of illness.[1,3] Terao *et al.* indicated that the clinical disease form may be a determining factor for neuronal loss in ALS spinal gray matter and that a marked depopulation of small neurons in spinal ventral horns could be observed in the pseudopolyneuritic form of ALS.[6]

We previously reported that the diffuse myelin pallor in the ventral aspects of anterolateral columns outside corticospinal tracts in ALS spinal cords might originate from degenerating anterior and lateral propriospinal bundles.[7] The neurons projecting to the anterior and lateral propriospinal bundles were reported to be small and located in the medial parts of the anterior horns, intermediate parts between anterior and posterior horns, and basal parts of the posterior horns in humans.[8] These reports led to the speculation that the diffuse myelin pallor in the anterolateral columns outside the corticospinal tracts of ALS spinal cord may be due to the loss of small neurons in these areas of gray matter. To address this issue, we further examined the ALS spinal cords of half of the patients in our previous study.[7]

METHODS

A short summary of the clinical and pathological findings of 15 ALS patients is shown in Table 1. The case numbers are the same as those assigned to patients in our previous report.[7] Among these patients, seven (5, 8, 22, 24, 27, 29, 30 in Table 1) had been artificially ventilated during the later stage of their illness. We also examined five control subjects (66 years/male, 55 years/female, 67 years/male, 96 years/female, 34 years/male) without spinal cord involvement.

Correspondence: Shintaro Hayashi, MD, PhD, Department of Neurology, Gunma University, Graduate School of Medicine, 3-39-15, Showa-machi, Maebashi, Gunma 371-8511, Japan. Email: sintaroh@med.gunma-u.ac.jp

Received 6 April 2006; revised and accepted 24 June 2006.

Table 1 Clinical and pathological findings of the ALS patients

Case	Age (years)	Sex	Duration	Respirator	MP
2	79	M	5 months	–	–
19	60	M	3 years 5 months	–	–
21	60	M	4 years	–	–
23	67	F	6 years	–	–
25	57	F	7 years	–	–
5	43	F	1 year	+ (15 days)	+
8	58	M	3 years	+ (2 years)	+
20	57	M	3 years 7 months	–	+
22	63	F	6 years	+ (3 years)	+
30	52	M	14 years	+ (11 years)	+
12	53	F	2 years 1 month	–	++
16	61	F	2 years 7 months	–	++
24	41	F	7 years	+ (2 years 5 months)	++
27	37	F	8 years 11 months	+ (7 years)	++
29	57	M	11 years 3 months	+ (10 years)	++

MP; myelin pallor. The case numbers are the same as those assigned to the patients in our previous report.[7]

The mid-portion of the thoracic cords were fixed in 10% buffered formalin solution and processed for paraffin-embedded transverse sections. For the detection of diffuse myelin pallor in the ventral aspects of the anterolateral columns and the quantitative analysis of neurons, KB staining was performed using six 6-μm thick serial sections observed under 400-fold magnification. Cells with minimal somal diameters <25 μm with fine Nissl granules and visible nucleoli were defined as small neurons.[1,9,10] The spinal gray matter was divided into four distinct areas based on a slight modification of the method used by Stephens *et al.*[11] The anteromedial part (AMP), intermediate parts (IMP) and posterior parts (PP) bilaterally were examined to quantify the number of small neurons,[8] as shown in Figure 1. We also quantified the number of large neurons in the anterolateral parts (ALP, Fig. 1), which were defined as having a multipolar shape and a minimal somal diameter >35 μm with dense staining for Nissl granules in the nucleolar plane.[12,13] Further, we counted the number of medium-sized neurons with a minimal diameter between 25 and 35 μm in the nucleolar plane found in AMP, IMP and PP. Double counting of the individual nucleolus of the large and medium-sized neuron was carefully avoided by comparing serial preparations with each other.

The number of small and medium-sized neurons was compared among ALS patients or between the ALS patients and control subjects. Large neurons were compared among ALS patients. Statistical evaluations were performed using unpaired *t*-test for comparison and $P < 0.05$ was considered significant. The results are represented as the average ± SD.

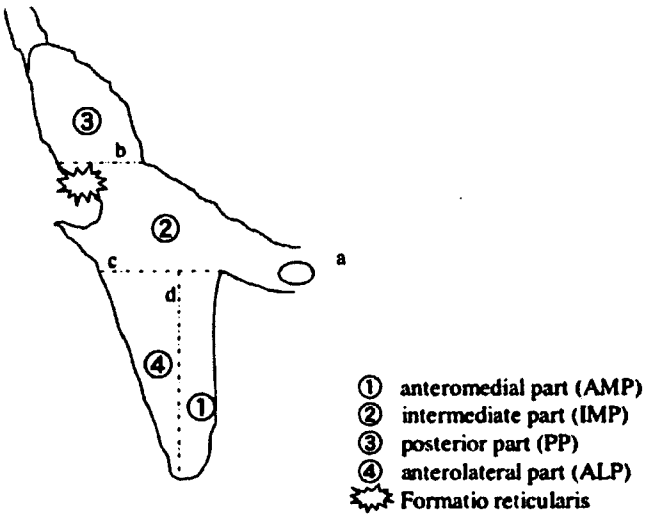

Fig. 1 The spinal gray matter was divided into four distinct areas, based on a slight modification of the method used by Stephens *et al.*[11] Based on the graticule observed in the microscopic field, line (a) is drawn horizontally starting from the central canal. Line (b) is drawn horizontally to line (a) through the upper margin of the formatio reticularis. Line (c) is drawn horizontally to line (a). Line (d) is drawn vertically to line (c) and linked with the apex of the anterior horn. The area encompassed by line (c), line (d) and the medial margin or lateral margin of the anterior horn is designated the anteromedial part (AMP) or anterolateral part (ALP), respectively. The area encompassed by line (b) and line (c) is designated the intermediate part (IMP). The area encompassed by line (b) and the posterior horn is designated the posterior part (PP).

RESULTS

The intensity of KB staining in the ventral aspects of anterolateral columns outside the corticospinal tracts of ALS spinal cords was classified into three categories as follows: (i) MP–, intensity similar to that of posterior columns (Fig. 2b); (ii) MP++, intensity was markedly decreased, as shown in Figure 2d, and corticospinal tracts were also severely degenerated in these cases (Fig. 2d); and (iii) MP+, intensity was intermediate between that of MP– and MP++, as shown in Figure 2c.

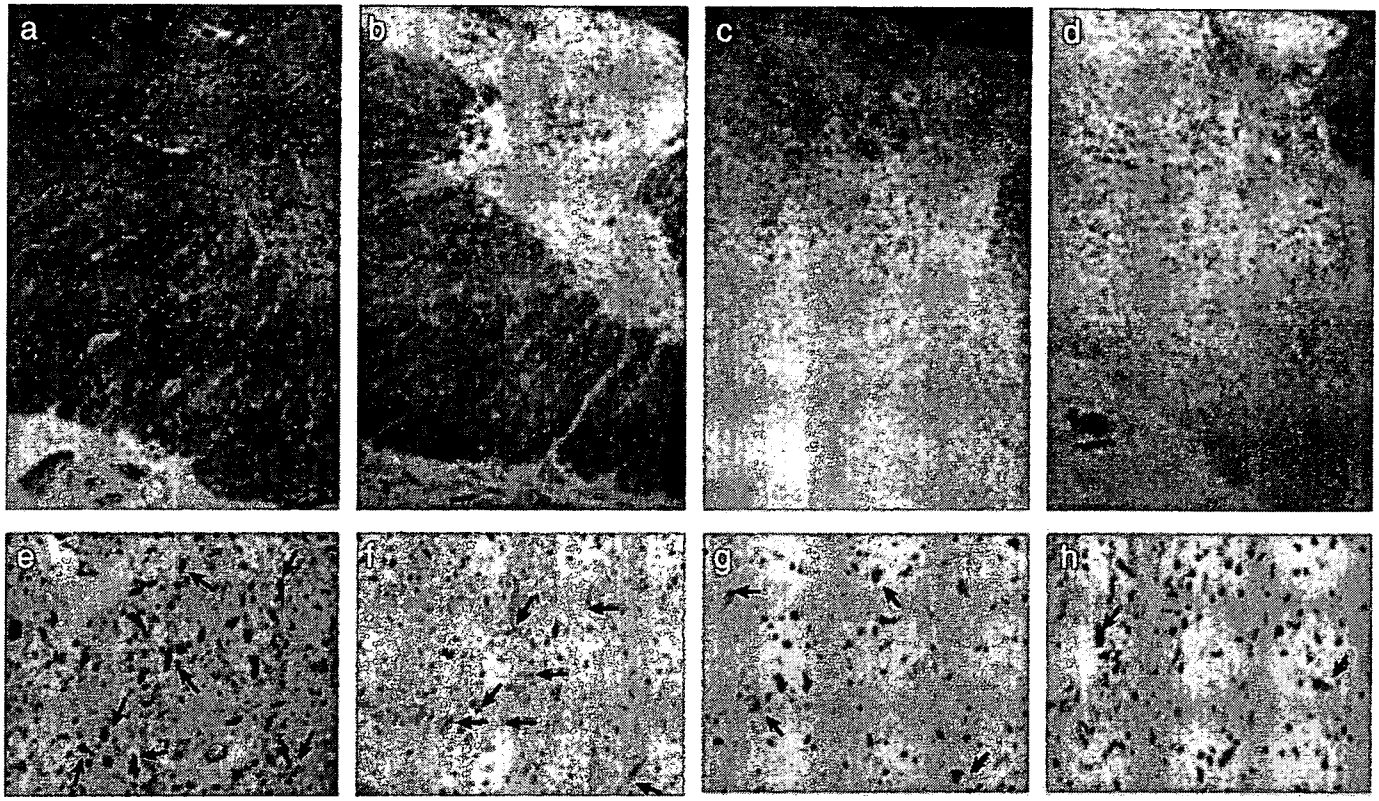

Fig. 2 (a–d) Light microscopy of the ventral aspects of the anterolateral columns in thoracic cords. (e–h) Large magnification of light microscopy showing intermediate parts (IMP) in each case. (a,e) Control subject; (b,f) ALS spinal cord of MP– (case 25); (c,g) MP+ (case 20) and (d,h) MP++ (case 16). Arrows indicate each small neuron, which is defined as a cell with a minimal somal diameter <25 μm with fine Nissl granules and a visible nucleolus. The numbers of small neurons in (f) are almost the same as those shown in (e). (g,h) Decreases in the numbers of small neurons, depending on the degree of the myelin pallor (compare c,d with a or b). KB staining. MP–, intensity of KB staining in the ventral aspect of anterolateral columns outside corticospinal tracts similar to that of the posterior columns; MP++, intensity markedly reduced to the same degree as that of severely degenerated corticospinal tracts; MP+, intensity intermediate between that of MP– and MP++.

First, we examined 100 small neurons in each control spinal cord and confirmed that there was no doubly counted nucleolus at this specimen thickness. Light microscopically, the number of small neurons in AMP and in IMP seemed to be almost the same between the control (Fig. 2e, arrows) and MP– (Fig. 2f, arrows) spinal cords. However, in the spinal cords of MP+ and MP++, the number of small neurons in these areas (Fig. 2g,h; arrows) appeared to be reduced depending on the degree of myelin pallor. To investigate whether this reduction was significant, we performed further quantitative and statistical analysis (Table 2). In AMP and in IMP, there were significant decreases of small neurons between the control and MP+ or between the control and MP++ spinal cords (control vs MP+, $P < 0.01$; control vs MP++, $P < 0.01$); but there were no significant differences in either area between the control and MP– spinal cords. The duration of illness did not differ significantly among MP–, MP+ and MP++, but the numbers of small neurons in AMP and in IMP decreased significantly in relation to intensity of myelin pallor (AMP: MP– vs MP+, $P < 0.01$; MP– vs MP++, $P < 0.01$; MP+ vs MP++, $P < 0.03$; IMP: MP– vs MP+, $P < 0.01$; MP– vs MP++, $P < 0.01$; MP+ vs MP++, $P < 0.01$). In PP, there were no significant differences in the number of small neurons between the ALS spinal cords and the controls.

Table 2 No. small neurons in each division at thoracic cords (mean ± SD)

	AMP	IMP	PP
Control ($n = 5$)	19.0 ± 3.6	83.0 ± 12.6	99.6 ± 10.2
MP– ($n = 5$)	17.2 ± 4.1	71.0 ± 12.9	115.0 ± 18.2
MP+ ($n = 5$)	7.4 ± 4.0[a,b]	46.0 ± 7.0[f,g]	91.4 ± 22.4
MP++ ($n = 5$)	1.6 ± 1.5[c,d,e]	27.6 ± 9.4[h,i,j]	97.6 ± 27.3

[a]Control vs MP+, $P < 0.01$; [b]MP– vs MP+, $P < 0.01$; [c]control vs MP++, $P < 0.01$; [d]MP– vs MP++, $P < 0.01$; [e]MP+ vs MP++, $P < 0.03$; [f]control vs MP +, $P < 0.01$; [g]MP– vs MP+, $P < 0.01$; [h]control vs MP++, $P < 0.01$; [i]MP– vs MP++, $P < 0.01$; [j]MP+ vs MP++, $P < 0.01$.

AMP, anteromedial portions; IMP, intermediate portions; MP, myelin pallor; PP, posterior portions.

We also quantified a number of the large anterior horn cells in ALP of the spinal cords of MP–, MP+ and MP++ (Table 1) and the results were 0.4 ± 0.6, 0.6 ± 0.6 and 0.4 ± 0.9, respectively (not significantly different among the

three categories). The large anterior horn cell : small neuron ratio in the control thoracic cords in the present study was 1:61.

In addition, we counted the number of medium-sized neurons in AMP, IMP and PP in the controls and ALS spinal cords and there were no significant quantitative differences in each division among the ALS patients and controls (data not shown).

DISCUSSION

Although approximately 100 years have elapsed since Holmes identified the degeneration of small neurons in ALS spinal gray matter,[14] little attention has been paid to this pathology and the precise mechanism leading to the loss of small neurons has not yet been resolved.[1-5] Several studies have reported that one of the possible determining factors for the reduction of small neurons was a long clinical course;[1-3] but the loss of Clark's column neurons or intermediolateral neurons was also observed in long-term ALS patients.[15-17] These reports suggest that a distinct factor other than a long clinical duration may promote the degeneration of small neurons in ALS spinal gray matter.

We considered that some problems in previous studies concerning the loss of small neurons in ALS spinal gray matter are as follows: (i) the results of the studies were based on so few cases that the significance of differences in the number of small neurons among ALS patients was not examined;[3,6] (ii) although many small neurons are distributed outside the anterior horns, the reports usually examined only the interior gray matter of anterior horns in ALS;[6,18] (iii) the definition of the anatomical locations were not consistent among studies, for example, Terao *et al.* defined the intermediate zone as the "dorsomedial portion of the anterior horn" in lumbar cords,[6] while Oyanagi *et al.* defined the intermediate zone as "Rexed's laminae V–VIII" in cervical cords.[3] To avoid these problems, we performed statistical analyses and examined almost all of the gray matter referring to the recent topographical analysis[11] for the quantification of small neurons in ALS spinal cord. The use of Rexed's criteria[19] was not attempted in the present study because the cytoarchitectural boundaries tend to be unstable in diseased spinal cords such as that in ALS.[11]

The present study showed that although there were no significant differences in the number of small neurons in AMP and in IMP between ALS spinal cords without the diffuse myelin pallor in the ventral aspects of anterolateral columns and the controls, reduction in the number of small neurons in these areas was significant in ALS spinal cords with diffuse myelin pallor compared to that in controls. Among ALS spinal cords, the numbers of small neurons in AMP and in IMP were decreased significantly in relation to the intensity of diffuse myelin pallor. Interestingly, the areas (AMP and IMP) in which a significant reduction of small neurons was observed in ALS spinal cords with the diffuse myelin pallor are compatible with the regions in which the cells projecting to the anterior and lateral propriospinal bundles are located.[8] There was no evidence of correlation between the number of medium-sized neurons in AMP, IMP and PP and the myelin pallor of the anterolateral columns in ALS spinal cord. These findings strongly suggest that diffuse myelin pallor in the ventral aspects of the anterolateral columns outside the corticospinal tracts in the ALS spinal cord might originate from a loss of small neurons in AMP and in IMP. These results may further support our previous proposal that diffuse myelin pallor in the ventral aspects of the anterolateral columns might originate from degenerating anterior and lateral propriospinal bundles.[7]

Previous studies reported other candidates for the origin of diffuse myelin pallor in the anterolateral columns of ALS spinal cords. Oyanagi *et al.* showed that large myelinated fibers were significantly reduced in the anterolateral columns of cervical segments in patients with lesions of pontine tegmentum.[20] They also showed in another study that in the anterolateral columns of ALS cervical segments, the number of large and medium-sized myelinated fibers were reduced.[21] They compared these manifestations and speculated that one of the candidates for the origins of degenerated large myelinated fibers in the anterolateral columns of ALS spinal cords was the pontine tegmentum.[20] Ikuta *et al.* reported that when the reticular formation was selectively degenerated in the case of sleep apnea syndrome, it induced myelin pallor in the anterolateral columns except for the corticospinal tracts, which was similar with the finding observed in the anterolateral columns of ALS spinal cords.[22] These findings suggested that myelin pallor in the anterolateral columns of ALS spinal cords might be derived from degeneration of the reticular formation. However, in two cases of motor neuron disease (spinal progressive muscular atrophy and ALS), which showed myelin pallor in the anterolateral columns outside corticospinal tracts of spinal cords, there was no evidence for the degeneration of reticular formation.[23] The precise origin of degenerated axons in the ventral aspects of anterolateral columns of ALS spinal cords has not yet been clarified, and further studies to investigate this issue may clarify the degenerating neuronal populations other than motor neurons involved in the pathology of ALS.

It remains to be resolved whether the decrease in small neurons occurs initially or subsequent to the loss of large anterior horn cells in ALS spinal gray matter. Some experiments using animals offer a potential avenue to clarify the relationship between small and large neuronal reduction in spinal cords. A study involving axotomy, which resulted in

the retrograde degeneration of large anterior horn cells in the rat spinal gray matter, indicated that there was no loss of small neurons in Rexed's laminae VII–X, even after the number of large anterior horn cells was found to have an 81% reduction.[24] However, in a transgenic mouse model of familial ALS, the large anterior horn cells at the end-stage were seen to have a 50–66% reduction,[25–27] and the loss of small neurons was also detected at this stage.[27] Morrison *et al.* reported that the loss of small neurons in laminae VII–X occurred in parallel to the loss of large anterior horn cells in a transgenic mouse model of familial ALS, implying that both cell types may be targets for the degenerative process.[27] Histological studies of muscle spindles in motor neuron disease showed that gamma motor innervation of the intrafusal muscle fibers was strongly involved, in parallel with changes in the alpha innervation of the extrafusal muscle fibers.[28,29] These studies suggest that the loss of small neurons in the spinal gray matter of ALS patients may originate from their intrinsic abnormalities.

Most of the small neurons located in IMP and AMP are thought to be interneurons.[4,11] The interneurons contact motor neurons,[30,31] other interneurons[32] and also project both intra- and intersegmentally as well as to the contralateral spinal cord.[33,34] Recently there has been emerging evidence that interneurons might be involved in ALS patients[4,11] and in transgenic mouse models of familial ALS;[23] but how this manifestation will modify the disease progression remains unclear. Stephens *et al.* speculated that the mode of the disease might relate to the major loss of spinal interneurons in ALS[11] because ALS first progresses clinically to contiguous areas, with symptom progression in segments (e.g., leg to contralateral leg) occurring more quickly and to a greater extent than symptom progression in the proximo-distal axis (e.g., leg to ipsi- or contralateral arm).[35] This is compatible with the progression of ALS along the distribution of interneuronal networks in the spinal cord.[36,37]

Further study is required to examine how interneuronal populations, excitatory, inhibitory or both types, are involved in ALS spinal cords and how their degeneration affects the clinical manifestations of ALS patients.

ACKNOWLEDGMENT

This work was supported by a grant from the Ministry of Health, Labour and Welfare of Japan to K. Okamoto.

REFERENCES

1. Tsukagoshi H, Yanagisawa N, Oguchi K *et al.* Morphometric quantification of the cervical limb motor cells in various neuromuscular disease. *J Neurol Sci* 1979; **41**: 287–297.
2. Oyanagi K, Makifuchi T, Ikuta F. A topographic and quantitative study in human spinal gray matter, with special reference to their changes in amyotrophic lateral sclerosis. *Biomed Res* 1983; **42**: 211–224.
3. Oyanagi K, Ikuta F, Horikawa Y. Evidence for sequential degeneration of the intermediate zone of the spinal cord in amyotrophic lateral sclerosis: A topographic and quantitative investigation. *Acta Neuropathol (Berl)* 1989; **77**: 343–349.
4. Swash M, Leader M, Brown A *et al.* Focal loss of anterior horn cells in the cervical cord in motor neuron disease. *Brain* 1986; **109**: 939–952.
5. Mizusawa H, Hirano A, Shintaku M. Involvement of small-sized neurons in anterior horn of the spinal cord in amyotrophic lateral sclerosis. *Neurol Med (Tokyo)* 1987; **27**: 331–336.
6. Terao S, Sobue G, Hashizume Y *et al.* Disease specific patterns of neuronal loss in the spinal ventral horn in amyotrophic lateral sclerosis, multiple system atrophy and X-linked recessive bulbospinal neuropathy, with special reference to the loss of small neurons in the intermediate zone. *J Neurol* 1994; **241**: 196–203.
7. Hayashi S, Sakurai A, Amari M *et al.* Pathological study of the diffuse myelin pallor in the anterolateral columns of the spinal cord in amyotrophic lateral sclerosis. *J Neurol Sci* 2001; **188**: 3–7.
8. Nathan PW, Smith MC. Fasciculi proprii of the spinal cord in man. *Brain* 1959; **82**: 610–668.
9. Jankowska E, Lindstrom S. Morphological identification of Renshaw cells. *Acta Physiol Scand* 1971; **81**: 428–430.
10. Kawamura Y, Peter JD. Permanent axotomy by amputation results in loss of motor neurons in man. *J Neuropathol Exp Neurol* 1981; **40**: 658–666.
11. Stephens B, Guiloff RJ, Roberto N *et al.* Widespread loss of neuronal populations in the spinal ventral horn in sporadic motor neuron disease. A morphometric study. *J Neurol Sci* 2006; **244**: 41–58.
12. Tomlinson BE, Irving D, Rebeiz IJ. Total numbers of limb motor neurons in the human lumbosacral cord and an analysis of the accuracy of various sampling procedures. *J Neurol Sci* 1973; **20**: 313–327.
13. Kawamura Y, Peter O, Okazaki H *et al.* Lumbar motor neurons of man II: The number and diameter distribution of large- and intermediate diameter cytons in motor neuron columns of spinal cord of man. *J Neuropathol Exp Neurol* 1977; **36**: 861–870.
14. Holmes G. The pathology of amyotrophic lateral sclerosis. *Rev Neurol Psychiatry* 1909; **7**: 693–725.
15. Takahashi H, Oyanagi K, Ohama E *et al.* Clarke's column in sporadic amyotrophic lateral sclerosis. *Acta Neuropathol (Berl)* 1992; **84**: 465–470.

16. Paul A, Paul C. Regular involvement of Clarke's nucleus in sporadic amyotrophic lateral sclerosis. *Arch Neurol* 1982; **39**: 155–156.
17. Takahashi H, Oyanagi K, Ikuta F. The intermediolateral nucleus in sporadic amyotrophic lateral sclerosis. *Acta Neuropathol (Berl)* 1993; **86**: 190–192.
18. Stephens B, Navarrete R, Guiloff RJ. Ubiquitin immunoreactivity in presumed spinal interneurons in motor neurone disease. *Neuropathol Appl Neurobiol* 2001; **27**: 352–361.
19. Rexed B. A cytoarchitechtonic atlas of the spinal cord in the cat. *J Comp Neurol* 1954; **100**: 297–379.
20. Oyanagi K, Kawakami E, Morita T *et al.* Pursuit of the origin of the large myelinated fibers of the anterolateral funiculus in the spinal cord in humans in relation to the pathomechanism in amyotrophic lateral sclerosis. *Acta Neuropathol (Berl)* 1999; **98**: 635–640.
21. Oyanagi K, Makifuchi T, Ikuta F. The anterolateral funiculus in the spinal cord in amyotrophic lateral sclerosis. *Acta Neuropathol (Berl)* 1995; **90**: 221–227.
22. Ikuta F, Makifuchi T, Ohama E *et al.* Tract degeneration of the human spinal cord: Some observation on ALS and hemispherectomized humans. *Shinkei Kenkyu no Shinpo* 1982; **26**: 710–736.
23. Hirayama K. Some problems of clinico-pathological study of motor neuron disease. *Psychiatr Neurol Jpn* 1962; **64**: 112–126.
24. Sharon MC, Lim RJ, Guiloff RN. Interneuronal survival and calbindin-D28K expression following motor neuron degeneration. *J Neurol Sci* 2000; **180**: 46–51.
25. Bruijn LI, Becher MW, Lee MK *et al.* ALS-linked SOD1 mutant G85R mediates damage to astrocytes and promotes rapidly progressive disease with SOD1-containing inclusions. *Neuron* 1997; **18**: 327–338.
26. Chiu AY, Zhai P, Dal Canto MC *et al.* Age-dependent penetrance of disease in a transgenic mouse model of familial amyotrophic lateral sclerosis. *Mol Cell Neurosci* 1995; **6**: 349–362.
27. Morrison BM, Janssen WG, Jon WG *et al.* Time course of neuropathology in the spinal cord of G86R superoxide dismutase transgenic mice. *J Comp Neurol* 1998; **391**: 64–77.
28. Swash M, Fox KP. The pathology of the muscle spindle: Effect of denervation. *J Neurol Sci* 1974; **22**: 1–24.
29. Swash M, Schwartz MS. A longitudinal study of changes in motor units in motor neuron disease. *J Neurol Sci* 1982; **56**: 185–197.
30. Eccles JC, Eccles RM, Lundberg A. Types of neurone in and around the intermediate nucleus of the lumbosacral cord. *J Physiol* 1960; **154**: 89–114.
31. Ellaway PH. Recurrent inhibition of fusimotor neurons exhibiting background discharge in the decerebrate and the spinal cat. *J Physiol (Lond)* 1971; **216**: 419–439.
32. Hultborn H, Illert M, Santini M. Convergence on interneurones mediating the reciprocal Ia inhibition of motorneurones: I. Disynaptic Ia inhibition of Ia inhibitory interneurones. *Acta Physiol Scand* 1976; **96**: 193–201.
33. Harrison PJ, Jankowska E, Zytnocki D. Lamina VIII interneurones interposed in crossed reflex pathways in the cat. *J Physiol* 1986; **371**: 147–166.
34. Fyffe RE. Spatial distribution of recurrent inhibitory synapses on spinal motorneurones in the cat. *J Neurophysiol* 1991; **65**: 1134–1149.
35. Brooks BR, Lewis D, Rawling J. *et al.* The natural history of amyotrophic lateral sclerosis. In: Williams AC (ed.). *Motor Neuron Disease*. London: Chapman & Hall, 1994; 131–169.
36. Jankowska E. Interneuronal relay in spinal pathways from proprioceptors. *Prog Neurobiol* 1992; **38**: 335–378.
37. Conradi S, Ronnevi LO. Selective vulnerability of alpha motor neurons in ALS: Relation to autoantibodies to acetylcholinesterase (AchE) in ALS patients. *Brain Res Bull* 1993; **30**: 369–371.

ELSEVIER

Journal of the Neurological Sciences 256 (2007) 10–20

Journal of the Neurological Sciences

www.elsevier.com/locate/jns

Nonapoptotic cell death caused by the inhibition of RNA polymerase disrupts organelle distribution

Shintaro Hayashi, Tsuneo Yamazaki , Koichi Okamoto

Department of Neurology, Gunma University, Graduate School of Medicine, 3-39-15 Showa-machi, Maebashi, Gunma 371-8511, Japan

Received 26 May 2006; received in revised form 18 January 2007; accepted 23 January 2007
Available online 23 March 2007

Abstract

It is controversial whether the mode of cell death induced by CAG repeat diseases is apoptotic. One technical problem that affects this issue is that the very methods used for DNA injection may induce artificial apoptosis. A recent study demonstrated that the functions of RNA polymerase II are disrupted in spinocerebellar ataxia type 1 (SCA 1) pathology, one of the CAG repeat diseases, and that -amanitin can inhibit the activity of RNA polymerase. To examine the cell death mechanisms involved in CAG repeat diseases, we treated cultured rat neurons with -amanitin to avoid the artifacts caused by DNA transfection. Mature and immature rat neurons were treated with -amanitin for 4–6 days and the effects of the treatment on the elongation of neurites, the distribution or morphology of organelles, and the nature of cell death were assessed by immunocytochemistry and quantitative analysis. Neurons exhibited a disruption of neurite elongation and eventually died by day 15 of the treatment. However, apoptosis was not detected. When the neurons survived well, but showed altered neurites, Golgi complexes and lysosomes exhibited changes in their normal intracellular distribution or morphology, but the endoplasmic reticulum and mitochondria did not. The distribution of phosphorylated Trk receptors was also disrupted in the neurites of treated neurons. The signal intensity of the dynein intermediate chain was markedly decreased in the treated neurons. Thus, organelle transport systems, particularly a minus-end-directed microtubule-dependent pathway, would be disrupted by the inhibition of RNA polymerase, and this change is likely to be an early event involved in SCA 1 pathology.

Keywords: Apoptosis; -Amanitin; Cultured neurons; Neuronal cell death; RNA polymerase; Golgi granulation; Lysosome dispersion

1. Introduction

The CAG repeat diseases include nine hereditary neurodegenerative disorders, Huntington disease (HD), dentatorubral–pallidoluysian atrophy, spinobulbar muscular atrophy and spinocerebellar ataxia (SCA) types 1, 2, 3, 6, 7, and 17. They are caused by the expansion of CAG triplet repeats in the genes encoding for a polyglutamine tract in normal protein. The precise mechanism leading to neuronal cell death in these disorders remains to be elucidated. Previous studies in vitro have highlighted the apoptosis involved in the mechanism of neuronal cell death in some CAG repeat diseases [1,2]. However, in the brains of human diseases, evidence of apoptotic neuronal death is scarce [3]. To study the mechanism of neuronal cell death in CAG repeat diseases, one problem to be solved is that overexpression systems using DNA transfection sometimes induce artificial apoptotic cell death, thus leading to misleading results [4]. Okazawa et al. [5] have now documented that, in the pathology of SCA 1, mutant ataxin-1 enhances the binding of polyglutamine tract binding protein-1 (PQBP-1) to the C-terminal domain of RNA polymerase II, which reduces the level of transcription. This report stimulated us to seek evidence of the cellular disturbance using the RNA polymerase inhibitor, -amanitin, in cultured neurons. This methodology has several advantages that can help avoid the artificial cell death caused by transfection, which may obscure the pathology of the disease. We found that this inhibitor induced nonapoptotic neuronal cell death over days, and altered the distribution of organelles

Corresponding author. Tel.: +81 272 20 8064; fax: +81 272 20 8068.
E-mail address: tsuneoy@med.gunma-u.ac.jp (T. Yamazaki).

0022-510X/$ - see front matter © 2007 Elsevier B V. All rights reserved.
doi:10.1016/j.jns.2007.01.077

ELSEVIER

Journal of the Neurological Sciences 256 (2007) 10–20

Journal of the Neurological Sciences

www.elsevier.com/locate/jns

Nonapoptotic cell death caused by the inhibition of RNA polymerase disrupts organelle distribution

Shintaro Hayashi, Tsuneo Yamazaki , Koichi Okamoto

Department of Neurology, Gunma University, Graduate School of Medicine, 3-39-15 Showa-machi, Maebashi, Gunma 371-8511, Japan

Received 26 May 2006; received in revised form 18 January 2007; accepted 23 January 2007
Available online 23 March 2007

Abstract

It is controversial whether the mode of cell death induced by CAG repeat diseases is apoptotic. One technical problem that affects this issue is that the very methods used for DNA injection may induce artificial apoptosis. A recent study demonstrated that the functions of RNA polymerase II are disrupted in spinocerebellar ataxia type 1 (SCA 1) pathology, one of the CAG repeat diseases, and that -amanitin can inhibit the activity of RNA polymerase. To examine the cell death mechanisms involved in CAG repeat diseases, we treated cultured rat neurons with -amanitin to avoid the artifacts caused by DNA transfection. Mature and immature rat neurons were treated with -amanitin for 4–6 days and the effects of the treatment on the elongation of neurites, the distribution or morphology of organelles, and the nature of cell death were assessed by immunocytochemistry and quantitative analysis. Neurons exhibited a disruption of neurite elongation and eventually died by day 15 of the treatment. However, apoptosis was not detected. When the neurons survived well, but showed altered neurites, Golgi complexes and lysosomes exhibited changes in their normal intracellular distribution or morphology, but the endoplasmic reticulum and mitochondria did not. The distribution of phosphorylated Trk receptors was also disrupted in the neurites of treated neurons. The signal intensity of the dynein intermediate chain was markedly decreased in the treated neurons. Thus, organelle transport systems, particularly a minus-end-directed microtubule-dependent pathway, would be disrupted by the inhibition of RNA polymerase, and this change is likely to be an early event involved in SCA 1 pathology.

Keywords: Apoptosis; -Amanitin; Cultured neurons; Neuronal cell death; RNA polymerase; Golgi granulation; Lysosome dispersion

1. Introduction

The CAG repeat diseases include nine hereditary neurodegenerative disorders, Huntington disease (HD), dentatorubral–pallidoluysian atrophy, spinobulbar muscular atrophy and spinocerebellar ataxia (SCA) types 1, 2, 3, 6, 7, and 17. They are caused by the expansion of CAG triplet repeats in the genes encoding for a polyglutamine tract in normal protein. The precise mechanism leading to neuronal cell death in these disorders remains to be elucidated. Previous studies in vitro have highlighted the apoptosis involved in the mechanism of neuronal cell death in some CAG repeat diseases [1,2]. However, in the brains of human diseases, evidence of apoptotic neuronal death is scarce [3]. To study the mechanism of neuronal cell death in CAG repeat diseases, one problem to be solved is that overexpression systems using DNA transfection sometimes induce artificial apoptotic cell death, thus leading to misleading results [4]. Okazawa et al. [5] have now documented that, in the pathology of SCA 1, mutant ataxin-1 enhances the binding of polyglutamine tract binding protein-1 (PQBP-1) to the C-terminal domain of RNA polymerase II, which reduces the level of transcription. This report stimulated us to seek evidence of the cellular disturbance using the RNA polymerase inhibitor, -amanitin, in cultured neurons. This methodology has several advantages that can help avoid the artificial cell death caused by transfection, which may obscure the pathology of the disease. We found that this inhibitor induced nonapoptotic neuronal cell death over days, and altered the distribution of organelles

Corresponding author. Tel.: +81 272 20 8064; fax: +81 272 20 8068.
E-mail address: tsuneoy@med.gunma-u.ac.jp (T. Yamazaki).

0022-510X/$ - see front matter © 2007 Elsevier B.V. All rights reserved.
doi:10.1016/j.jns.2007.01.077

37 °C for a further 30 min and then the medium was replaced with fresh prewarmed N2.1.

2.6. Labeling of lysosomes with LysoTracker Red DND-99

The control and -amanitin-treated neurons were incubated with prewarmed (37 °C) N2.1 medium containing LysoTracker Red DND-99 (25 nM) for 30 min, and then the medium was replaced with fresh prewarmed N2.1.

2.7. Quantitative analysis of neurite length

Neurons stained with anti-tubulin antibody were photographed, and total neurite length within a 0.04 mm^2 area was quantified with a curvimeter (Sakurai, Tokyo, Japan) under 1100-fold magnification. This assessment was performed for control neurons ($n=4$) and -amanitin-treated neurons ($n=4$) dissected on different days and the results were analyzed with the Mann–Whitney U test. $P<0.05$ was considered significant.

2.8. Cell viability assay and detection of apoptotic cells

Cell viability was analyzed using a LIVE/DEAD Viability/Cytotoxicity Kit (Molecular Probes) according to the manufacturer's instructions. Briefly, neurons were incubated in a mixture of 1 M ethidium homodimer-1 and 5 M calcein for 40 min at room temperature. Subsequently,

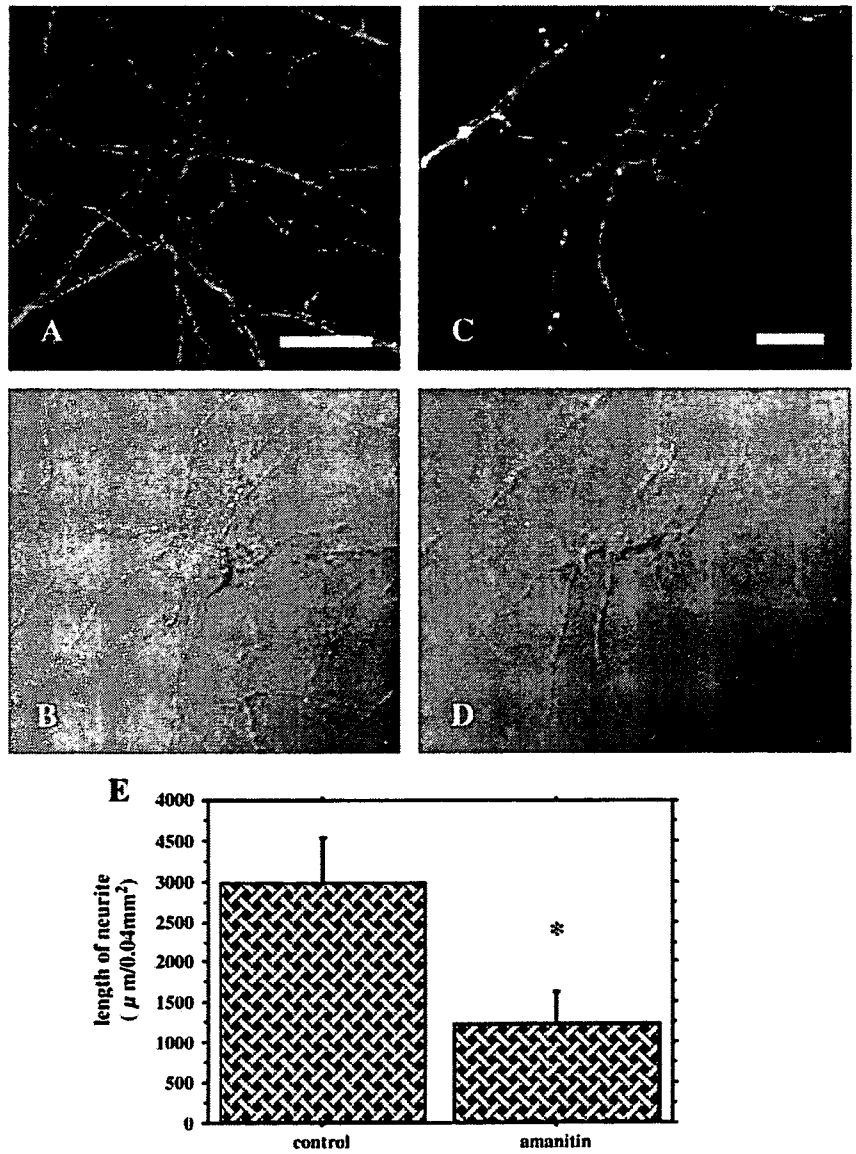

Fig. 2. Alpha-amanitin treatment altered neurite elongation in cultured neurons. Three-day-old hippocampal neurons were cultured with or without 2.5 M -amanitin for 6 days, and examined using anti-tubulin staining (A, C) and differential interference contrast images (B, D). Compared with the control (A, B), the treated neurons (C, D) demonstrated fewer neurites, but their tubulin was not disrupted (C). Quantitative analysis showed the neurites of the treated neurons to be significantly shorter than those of controls (E, $P<0.01$). Bars=10 m.

cover slips were mounted in the same solution and observed under a microscope using ultraviolet (UV) illumination. The numbers of live and dead neurons were counted on days 5, 7, 9 and 11 after the start of the -amanitin treatment, and the percentages of neurons that were dead on each day were determined. On the same days, the numbers of apoptotic cells were determined using an annexin-V-Fluos/propidium iodide (PI) detection kit (Roche Molecular Biochemicals, Mannheim, Germany). Neurons were considered apoptotic when they exhibited annexin-V positivity/PI negativity, since early apoptotic cells did not incorporate PI, while cells co-labeled with annexin-V and PI were considered necrotic [8]. The experiments were repeated three times and the data were first tested for normality of distribution, then analyzed using a one-way factorial analysis of variance (ANOVA) followed by unpaired Student's *t*-tests.

2.9. Treatment with brain-derived neurotrophic factor (BDNF)

Seven- to nine-day-old neurons, treated with -amanitin for 4 to 6 days, were stimulated with 1 nM BDNF (R&D Systems, Minneapolis, MN, USA) for 15 min at 37 °C in a 5% CO_2 incubator [9]. The neurons were then fixed as above and processed for double labeling using antiphosphorylated Trk receptors and anti-GM130 antibodies.

2.10. Western blotting

On the fifth day of -amanitin treatment, the control and -amanitin-treated neurons were lysed in sample buffer (80 mM Tris–HCl, pH 6.8, 10% glycerol, 2% SDS, and 1% 2-mercaptoethanol). The lysates were heated for 5 min at 100 °C and loaded on 5% polyacrylamide-SDS gels. After the electrophoresis, proteins were electrotransfered onto a PVDF membrane (MILLIPORE, MA, USA). The membrane was blocked in TST (50 mM Tris, 150 mM NaCl, and 0.1% Tween20, pH 7.6) containing 5% non-fat dry milk before incubation with the C-21 antibody. After multiple washes in TST, membranes were incubated with peroxidase-conjugated goat anti-rabbit IgG secondary antibody and washed again prior to visualization using ECL (Amersham, Buckinghamshire, UK) and Hyperfilm ECL (Amersham) exposure.

3. Results

3.1. Neuronal cell death induced by the RNA polymerase inhibitor

First, we aimed to determine whether the RNA polymerase inhibitor induced any morphological changes in the cultured cells. Previous studies demonstrated that the transcription of RNA was inhibited by -amanitin at 0.1–10 M in cultured rat cells [10]. Therefore, 3 days after plating, -amanitin was added to the culture medium at concentrations of 0, 0.1, 1, 2.5, and 10 M, and the treatment was continued for 5–15 days. On the fifth day of treatment, Western blot analysis revealed that the expression of one of the large subunits of RNA polymerase II (Rpb 2) was markedly decreased by -amanitin treatment compared to that of Rpb 1 (Fig. 1). RNA polymerase II is composed of several subunits [11]. Among them, the two large subunits of RNA polymerase II, Rpb 1 and Rpb 2, are essential for mRNA synthesis and Rpb 2 mutations can affect the stability of RNA polymerase II [11]. Therefore, Fig. 1 indicates that RNA transcription is impaired in cultured neurons by -amanitin treatment. Susceptibility to -amanitin differed among the subunits of RNA polymerase II [12], however, the reason for this difference remains unclear. During the first 5 days of the treatment, anti-tubulin staining did not differ between the control and treated neurons (Fig. 2A, C);

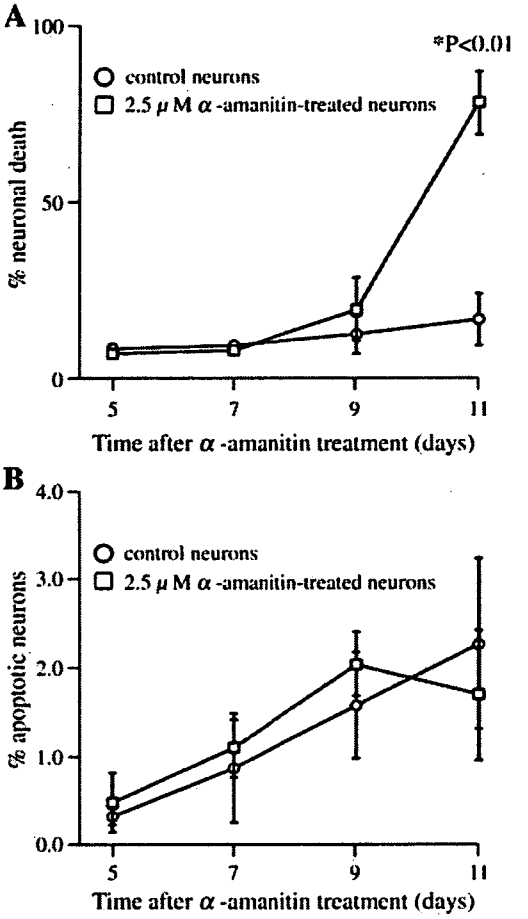

Fig. 3. Alpha-amanitin treatment induced neuronal cell death, but not apoptosis. (A) Three days after plating, neurons were cultured with or without 2.5 M -amanitin; dead cell numbers were determined on the indicated days. The percentage of dead cells increased significantly by the 11th day of treatment. Note that the proportion of dead cells was unchanged up to 9 days of treatment. (B) Three days after plating, neurons were cultured with or without -amanitin, and apoptotic cells were detected using the annexin-V-Fluos/propidium iodide system on the indicated days. The percentage of apoptotic cells was not significantly increased, even on the 11th day of treatment when cell death was apparent (compare with A). Each point represents the mean±SD of three separate experiments.

however, the elongation of neurites was affected by -amanitin at concentrations greater than 1 M (Fig. 2C, D) and neurites were significantly shorter than those of controls (Fig. 2E), suggesting that the -amanitin treatment altered neurite elongation, but that it was not caused by the disruption of microtubule assembly. Occasionally, the treatment also caused the dilatation of neurites (Fig. 8G, inset). However, even when neurite elongation was apparently affected, the majority of the neurons still survived for several more days with the treatment. Almost all of the neurons were dead after 15 days. These findings suggest that -amanitin induces neuronal cell death, but that this proceeds very slowly over several days. Treatments using 1.0, 2.5, and 10 M -amanitin produced identical results.

To quantify this death process, we determined the percentage of dead cells. We treated the neurons with 2.5 M -amanitin for different durations and counted the percentages of dead hippocampal neurons with or without treatment. In this study, the average numbers of control and treated neurons per coverslip were 517.5 and 498.4, respectively. As shown in Fig. 3A, the percentages of dead cells did not differ significantly between the control and RNA polymerase-inhibited cells until the ninth day of the treatment, even though the elongation of neurites in the treated neurons was apparently affected.

To determine whether the -amanitin-induced neuronal cell death was apoptotic, cultures were double stained with PI and annexin-V, an early marker of apoptosis [8]. As shown in Fig. 3B, the percentage of apoptotic neurons did not differ significantly between the control and treated cells, even by the 11th day of treatment, indicating that apoptotic mechanisms were not involved.

3.2. Distribution of organelle markers was affected by the RNA polymerase inhibitor in neurons

To analyze the death process induced by -amanitin, we first focused on observing the changes in the distribution of organelles in neurons. Cells at the six-day point were selected because at this time neurons were alive, but had altered neurites.

The distribution of Golgi complexes was examined using immunocytochemistry. In the control neurons, the antibody GM130, which recognizes Golgi matrix protein, stained ribbon-like structures located around the nuclei, which is consistent with a normal appearance and distribution of Golgi complexes (Fig. 4A). However, in the -amanitin-treated cells, the staining pattern became highly granulated and covered entire somata and neurites (Fig. 4E). The Golgi complexes did not intrude into all the neurites and were located mainly in the

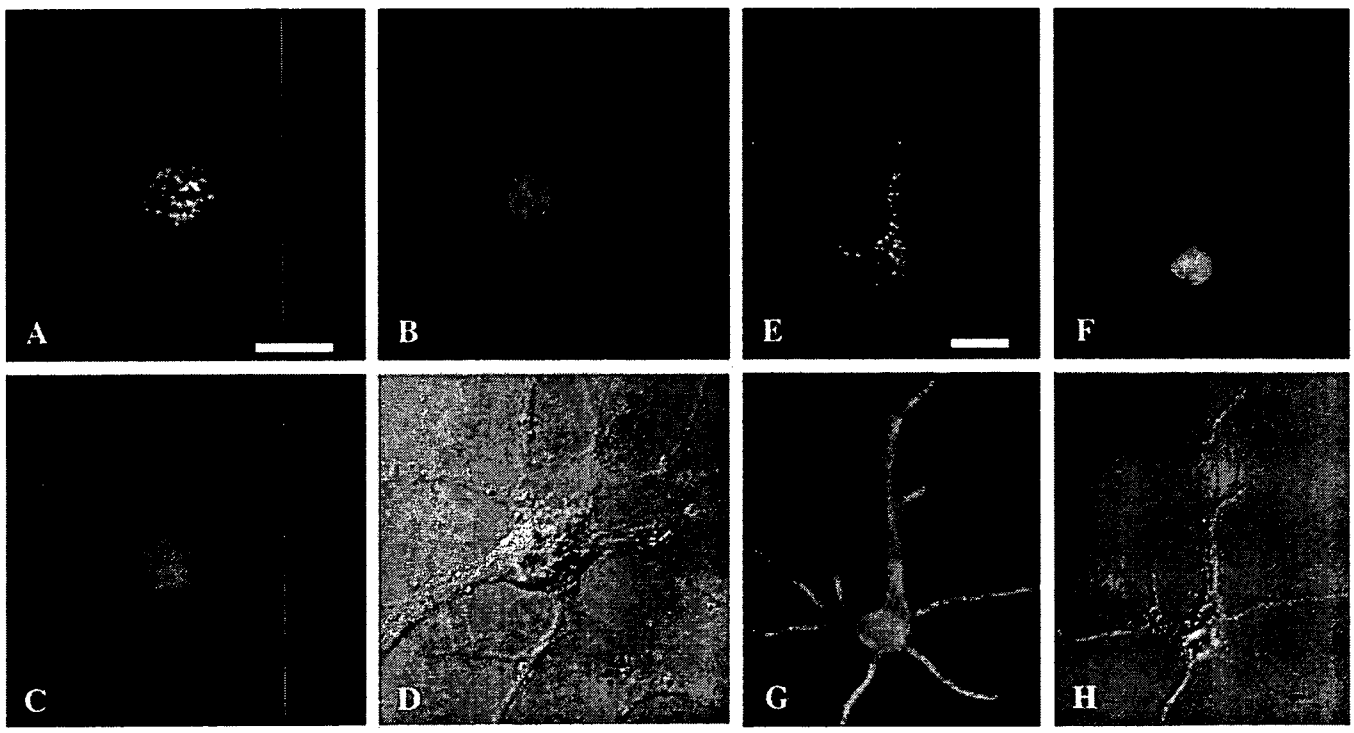

Fig. 4. Alpha-amanitin treatment altered the morphology and distribution of Golgi complexes. Three days after plating, neurons were treated with or without 2.5 M -amanitin. After 6 days of treatment, control (A–D) and treated (E–H) hippocampal neurons were labeled with GM130 (A, E), Hoechst 33258 (B, F), and MAP2 (C, G) staining and visualized using differential interference contrast microscopy (D, H). Compared with control neurons (A), Golgi complexes in the treated neurons (E) were granulated and dispersed, and some of their elements intruded into proximal parts of the neurites (compare E with G and H). Neurite elongation was disturbed (G, H), but there was no chromatin condensation (F) in the treated neuron. The total numbers of counted neurons at each time point were: [660, 410, 520 (control)/580, 490, 480 (treated neurons)]. The percentage of neurons with altered Golgi complexes was 0.1±0.2% in controls vs 99.0±1.7% in treated neurons ($P<0.01$). The consistent results were obtained using cortical neurons. Bars=10 m.

proximal parts of the processes. To confirm these findings, neurons were stained with another anti-Golgi antibody, TGN38 (Affinity BioReagents, Golden, CO, USA), that recognizes *trans*-Golgi protein. Similar results were obtained (data not shown). Nucleic acid staining showed no condensed nuclei in the treated neurons (Fig. 4F), thus confirming that the neurons were not undergoing apoptosis.

We also examined the distribution of lysosomes using the LAMP1 antibody. In control neurons, LAMP1 staining was evident as granular structures, mainly in the cell body, with some in neurites (Fig. 5A, B). In -amanitin-treated neurons, many of the LAMP1-positive signals were observed in cell bodies, but intense immunosignals were also detected in the proximal parts of long neurites (Fig. 5C, D).

To clarify whether the altered staining patterns observed in -amanitin-treated neurons are simply caused by changes in expression rather than distribution, we further observed the distribution of Golgi complexes and lysosomes using fluorescent probes (C5-DMB-Ceramide, which is a fluorescent sphingolipid and accumulates in the Golgi complex, and LysoTracker Red DND-99, which is an acidotrophic probe and accumulates in lysosomes). The results were consistent with those obtained with immunofluorescence microscopy (compare Fig. 6 with Figs. 4 and 5).

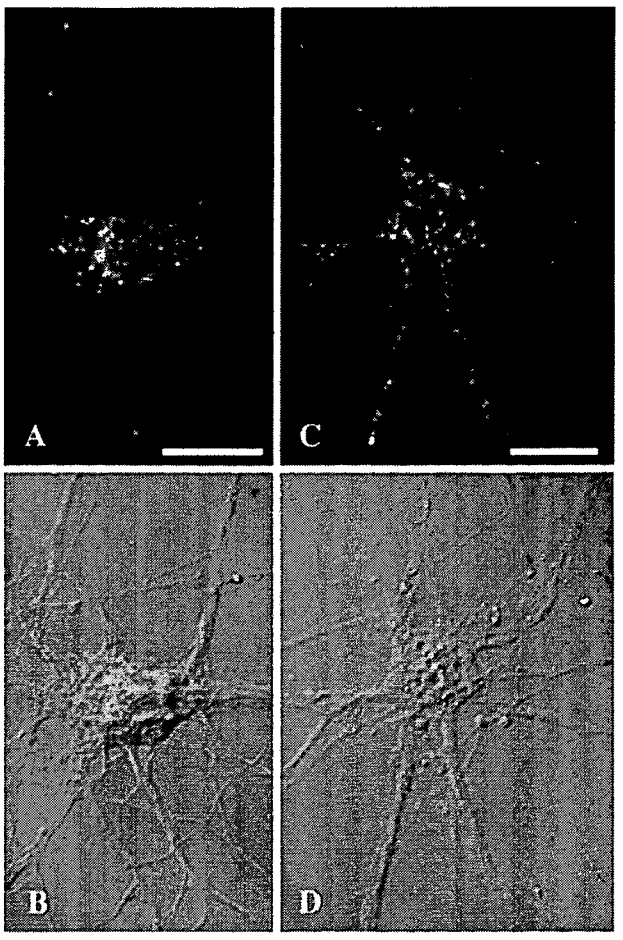

Fig. 5. Distribution of lysosomes was also disrupted by -amanitin treatment. Three days after plating, neurons were cultured with or without 2.5 M -amanitin. After 6 days of treatment, control (A, B) and treated (C, D) hippocampal neurons were labeled with LAMP1 (A, C) and visualized using differential interference contrast microscopy (B, D). LAMP1-positive lysosomes were dispersed and intruded into long neurites in treated neurons (C, D). The total numbers of counted neurons at each time point were: [600, 530, 420 (control)/590, 520, 490 (treated neurons)]. The percentage of neurons with altered lysosomes was 1.0±0.3% in controls vs 81.0±13.0% in treated neurons ($P<0.01$). Bars=10 m.

We further examined quantitatively whether these alterations to the Golgi complexes and lysosomes resulted from the -amanitin treatment. Percentages of neurons with altered Golgi complexes or lysosomes were calculated, and differences in the percentages between controls and treated neurons were analyzed using the Mann–Whitney U test with $P<0.05$ considered significant. The percentage of neurons with altered Golgi complexes was 0.1±0.2% in controls vs 99.0±1.7% in treated neurons ($P<0.01$) while that of neurons with altered lysosomes was 1.0±0.3% vs 81.0±13.0% ($P<0.01$). The percentage values indicate the mean±SD from three independent experiments. These results suggest that the distributional changes of Golgi complexes and lysosomes would be closely related to the -amanitin treatment.

We next examined the localization of the endoplasmic reticulum (ER) and mitochondria using anti-KDEL antibody and MitoTracker Green FM, respectively. As shown in Fig. 7A–D, the cellular distribution of neither set of organelles was affected by the -amanitin treatment.

All experiments were repeated with 14-day-old neurons. Treatment was started on the eighth day after plating; the incubation was continued for 6 days, and the results were consistent with the findings for both hippocampal and cortical neurons.

3.3. Distribution of pre- and postsynaptic markers was unaffected by the RNA polymerase inhibitor

We determined whether synaptic formation was altered by the treatment. Anti-synaptophysine antibody (SY38), which detects presynaptic terminals, and an anti-GluR1 antibody that labels postsynaptic sites were used. As shown in Fig. 7E–H, these pre- and postsynaptic markers exhibited fine granular staining in both untreated and treated neurons, indicating that synaptic localization and density were not altered by the -amanitin treatment.

3.4. Intra-axonal distribution of phosphorylated Trk receptors was altered by -amanitin treatment

Furthermore, we attempted to determine whether retrograde axonal transport was disturbed in the treated neurons. We examined the intra-axonal distribution of phosphorylated Trk receptors, which are known to be transported by retrograde axonal flow. In control neurons, there were numerous small stained granules in the axons, distributed evenly along the entire length (Fig. 8A). By contrast, this

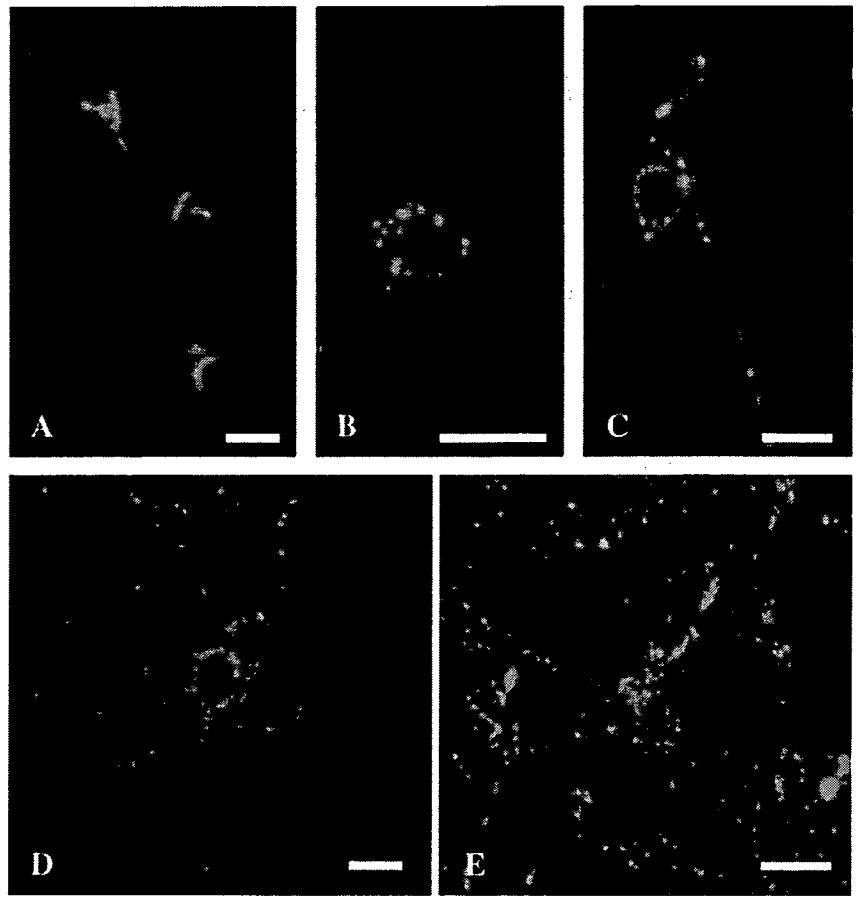

Fig. 6. Morphology or distributional alterations of Golgi complexes and lysosomes were observed by staining with BODIPY-C5-Ceramide and LysoTracker Red DND-99 stainings. Three days after plating, neurons were treated with or without 2.5 M -amanitin. After 5 days of treatment, control (A, D) and treated (B, C, E) cortical neurons were labeled with BODIPY-C5-Ceramide (A, B, C) and LysoTracker Red DND-99 (D, E). Compared to control neurons (A), Golgi complexes were granulated and dispersed over entire somata and neurites (B, C). Compared to controls (D), LysoTracker-positive granules were observed in cell bodies, but intense signals were also detected in neurites (E). The total numbers of counted neurons at each time point were: [510, 580, 490 (control)/600, 510, 530 (treated neurons)] for evaluation of Golgi complexes and [620, 540, 530 (control)/520, 450, 550 (treated neurons)] for evaluation of lysosomes. The percentage of neurons with altered Golgi complexes was 1.2±0.6% in controls vs 98.6±2.1% in treated neurons ($P<0.01$) while that of neurons with altered lysosomes was 1.6±0.5% vs 88.3±9.8% ($P<0.01$). Bars=10 m.

immunoreaction was not equally dispersed in -amanitin-treated neurons. A nonuniform distribution of phosphorylated Trk receptors was evident, especially in axons where Golgi complexes had accumulated. In all these axons, more receptors tended to be located in distal parts of the neurites (Fig. 8B, triangles), whereas fewer fluorescent signals were observed in the proximal parts (Fig. 8B, arrows), where Golgi complexes had accumulated (Fig. 8C, arrows). To confirm these findings, the distribution of phosphorylated Trk receptors was determined in the presence of exogenous BDNF, which intensifies both the phosphorylation [9] and the retrograde transport of TrkB [13]. As expected, there was less labeling of phosphorylated Trk in the proximal areas of neurites, where processes were expanded (Fig. 8G, triangle) and the Golgi complexes had accumulated, although bright signals were detected in the distal parts, where there was no such accumulation (Fig. 8E, F). These distributional changes to Golgi complexes and phosphorylated Trk receptors were not observed in control neurons.

3.5. DIC signal intensity was diminished in the -amanitin-treated neurons

Finally, we investigated immunocytochemically whether the signal for dynein was affected by the -amanitin treatment. The DIC signal was most intense in the perinuclear region in all of the control neurons (Fig. 9A); however, it was not detected in any of the -amanitin-treated neurons (Fig. 9C).

4. Discussion

There has been a long-running debate over whether the cell death involved in CAG repeat diseases is apoptotic [1,2,14]. Results obtained using cultured cell lines suggest that mutant forms of CAG repeat-coded proteins can cause neuronal cell death through a caspase-dependent mechanism that displays some of the features of apoptosis [2]. However, these studies reflect at best a poor approximation

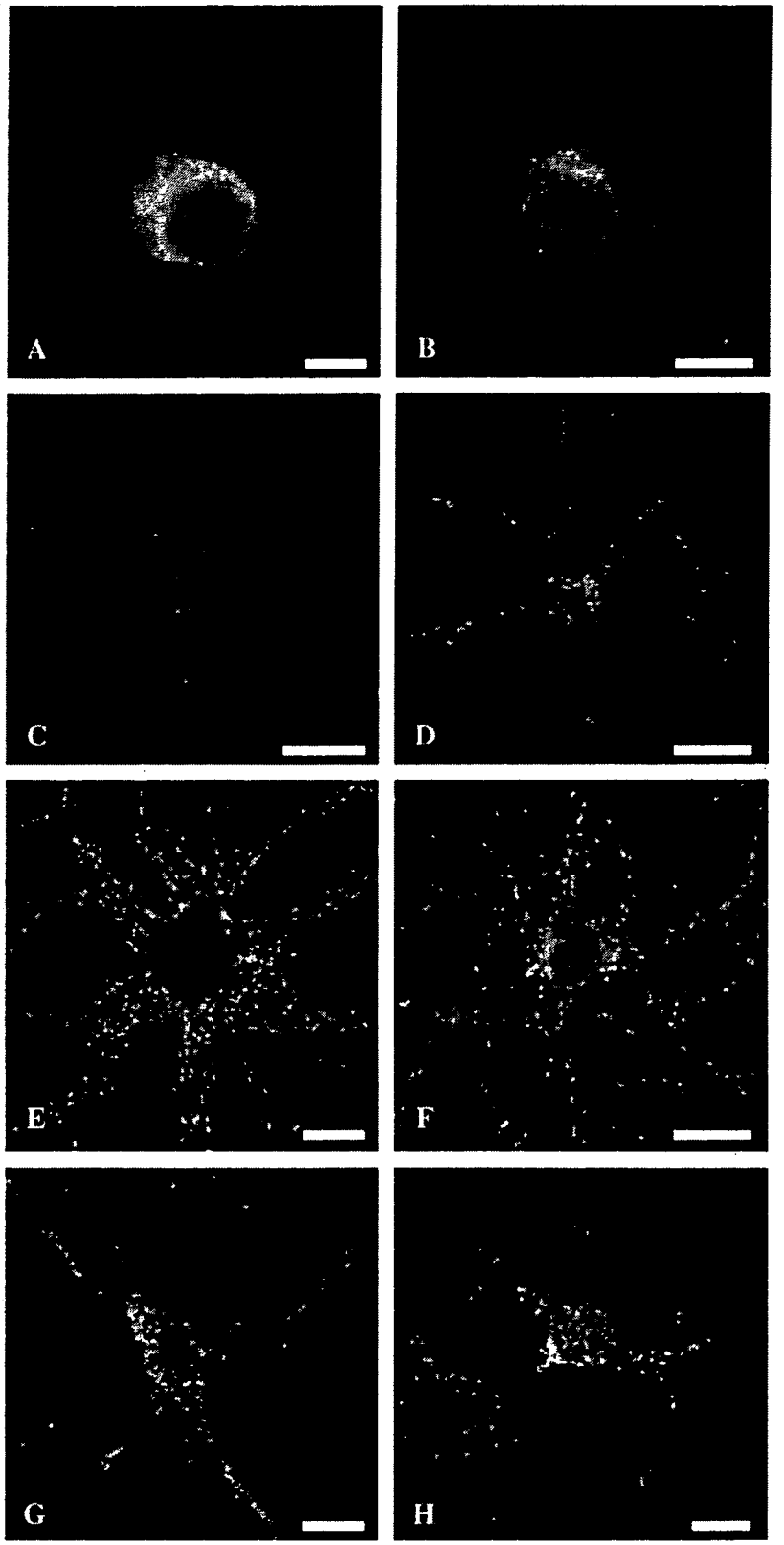

Fig. 7. Distributions of the endoplasmic reticulum (ER), mitochondria and synaptic markers were not altered by -amanitin treatment. Three days after plating, neurons were cultured with or without 2.5 M -amanitin. After 6 days of treatment, control (A, C, E, G) and treated (B, D, F, H) hippocampal neurons were labeled with anti-KDEL (A, B), SY38 (E, F), and GluR1 (G, H) antibodies and MitoTracker Green FM (C, D). The -amanitin treatment did not change the morphology or distribution of ER (B), mitochondria (D), presynaptic proteins (F) or postsynaptic proteins (H). The total numbers of counted neurons at each time point were: [610, 440, 480 (control)/600, 480, 460 (treated neurons)]. Panels A–F are epifluorescence images, and G and H were obtained by confocal laser microscopy. Bars = 10 m.

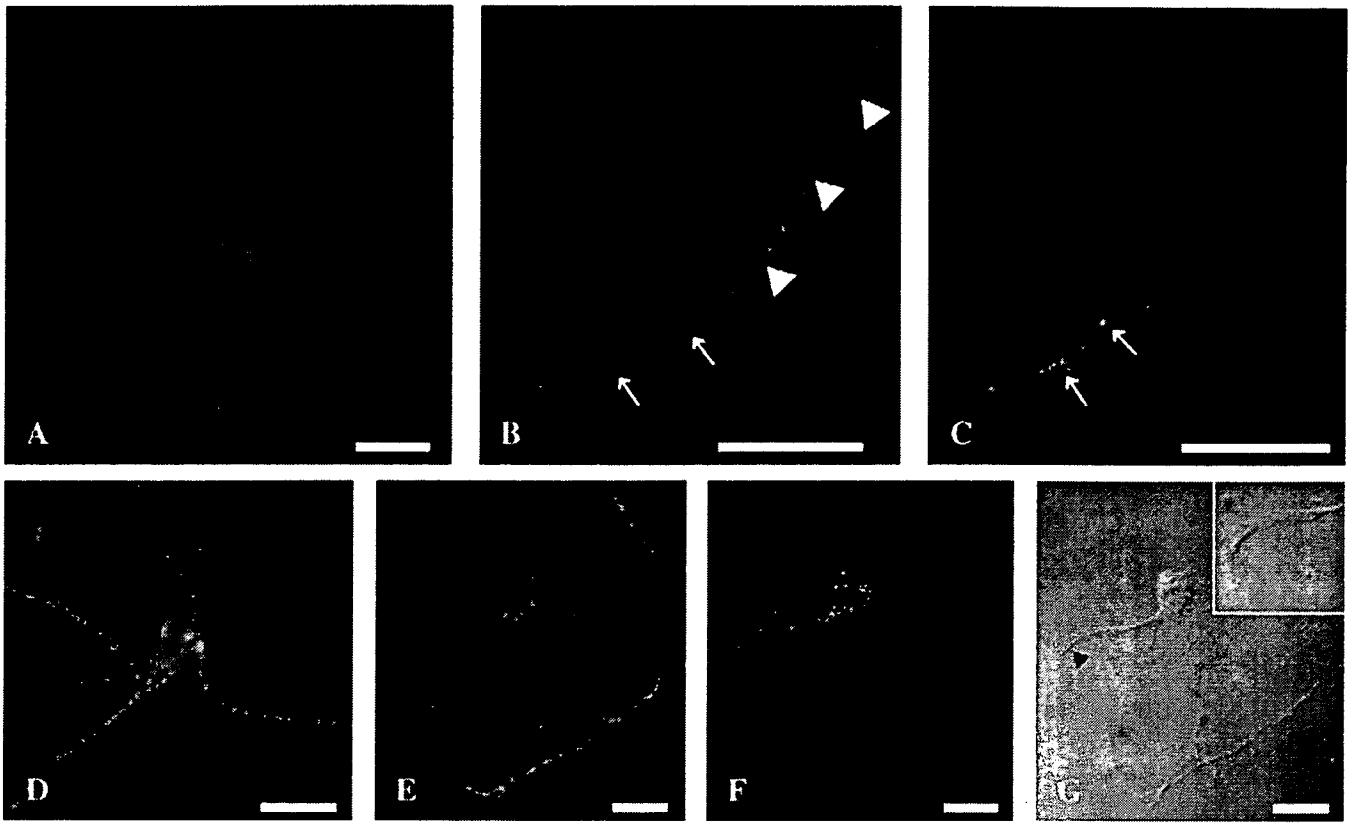

Fig. 8. Retrograde axonal transport might be altered by -amanitin treatment. Three days after plating, neurons were cultured with or without 2.5 M -amanitin. After 5 days of treatment, control (A, B, C, D) and treated (E, F, G) hippocampal neurons were labeled with phosphorylated Trk receptors and GM130 staining. In the control neurons, phosphorylated Trk receptors were distributed evenly along entire neurites (A). In the -amanitin-treated neurons (B), the immunopositive granules tended to be located in the more distal parts of the neurites (B: triangles) and were scarce proximally, where the Golgi complexes accumulated (B, C: arrows). For panels A–C, the total numbers of counted neurons at each time point were: [570, 420, 520 (control)/510, 570, 470 (treated neurons)]. 20.5±2.3% of the treated neurons had such axons as showing both altered Golgi complexes and nonuniformly distributed phosphorylated Trk receptors. These distributional changes to Golgi complexes and phosphorylated Trk receptors in axons were not observed in any of the control neurons. In the presence of 1 nM BDNF, many intense phosphorylated Trk signals were evident in the control neurons (D: compare with A). Proximal regions of the axon, where Golgi complexes accumulated (F) showed less labeling (E). At this site, a partial dilatation of the neurites was observed using differential interference contrast microscopy (G: triangle). The inset corresponds to an enlargement of the dilated portion of the neurite indicated by the triangle in G. For panels D–G, the total numbers of counted neurons at each time point were: [560, 520, 500 (control)/510, 560, 480 (treated neurons)]. 24.6±3.3% of the treated neurons had such axons as showing both altered Golgi complexes and nonuniformly distributed phosphorylated Trk receptors. These distributional changes to Golgi complexes and phosphorylated Trk receptors in axons were not observed in any of the control neurons. Bars = 10 m.

of human chronic diseases, such as HD and SCA 1, which progress over years, not hours. Kim et al. also showed that cloned striatal cells had an apoptotic morphology, even when transfected with the wild-type huntingtin protein [4]. Studies in animal models have also failed to resolve this issue. In some mouse models of HD, both terminal deoxynucleotidyl transferase Biotin-dUTP nick end labeling (TUNEL) and electron microscopy revealed apoptotic degenerative changes in the striatum [1]. In contrast, Turmaine et al. examined neurodegeneration both in a transgenic mouse model and in the brains of patients who had died of HD, and found no evidence supporting apoptotic neuronal cell death [14]. These results suggest that care is needed when interpreting the cell death induced by the overexpression of mutant protein. Recently, Okazawa et al. [5] showed that mutant ataxin-1 inhibited RNA polymerase II, which prompted us to use an RNA polymerase inhibitor, -amanitin, to avoid the artificial cell death caused by the transfection methodology, and investigated whether it could cause neuronal cell death. Treatment with -amanitin evidently induced neuronal degeneration, but this form of cell death occurred over a period of days, not hours. In addition, neither PI staining nor the annexin-V apoptosis detection system revealed increased apoptosis in -amanitin-treated neurons compared with the controls, suggesting the involvement of death mechanisms other than apoptosis. Okazawa et al. [5] also documented that transfection of mutant ataxin-1 produced cell death, and electromicroscopic examination revealed features of apoptosis. However, in their experiments, transfection of both empty vector and wild-type ataxin-1 also induced cell death, indicating that the apoptotic features observed in their experiments resulting from the cytotoxicity of mutant ataxin-1 or artificial events

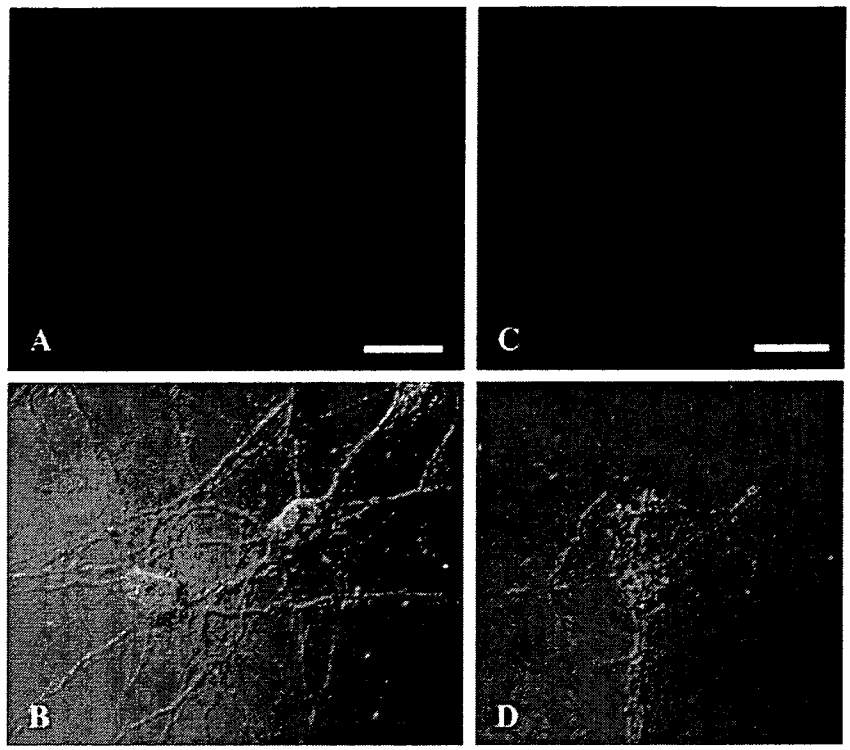

Fig. 9. Signal intensity of DIC was affected by the -amanitin treatment. Three days after plating, neurons were cultured with or without 2.5 M -amanitin. After 6 days of treatment, control (A, B) and treated (C, D) hippocampal neurons were labeled with DIC staining and visualized using differential interference contrast microscopy (B, D). In controls, DIC signal intensity was clearly detectable inside neurons, especially in the perinuclear region (A); however, in treated neurons, the signals were markedly decreased (C). The total numbers of counted neurons at each time point were: [600, 510, 520 (control)/550, 490, 500 (treated neurons)]. The DIC signal intensity was markedly decreased in all of the treated neurons, as shown in the panel (C). Bars=10 m.

were not clear. Rigorous investigations are clearly needed to elucidate the exact cell death mechanisms of polyQ diseases.

During the course of cell death, we found changes in the distribution of some organelles in treated neurons, but without any alterations in nuclear morphology or microtubule organization. Interestingly, the cellular distribution of both Golgi complexes and lysosomes was affected, but that of the ER and mitochondria was not. The Golgi complexes also became highly granulated. It is important to note that the dispersion patterns obtained in this study are similar to those seen when cytoplasmic dynein—a minus-end-directed microtubule-based motor protein—is disrupted [15]. Furthermore, we directly examined whether dynein expression was affected by the -amanitin treatment. The immunocytochemical results showed that DIC signal intensity was markedly decreased in treated neurons (Fig. 9C) compared with the controls (Fig. 9A). These findings suggest that the -amanitin treatment strongly downregulated the DIC expression. It is known that retrograde movements of the ER and mitochondria involve mechanisms other than the microtubule system [16,17], although those of Golgi complexes and lysosomes are totally microtubule-dependent [18,19]. Thus, the disruption to dynein has different effects on the distribution of organelles, depending on their requirements for microtubule transport. Because cytoplasmic dynein is also a key protein for retrograde axonal transport [20], these observations suggest that retrograde axonal flow might be disrupted in the treated neurons. To test this possibility, we examined the distribution of phosphorylated Trk receptors in -amanitin-treated neurons. Trk receptors in axonal ends are known to be transported back to the cell body by retrograde axonal transport after phosphorylation by binding with neurotrophic factors [9,13]. We found that the distribution of phosphorylated Trk receptors in axons was indeed disturbed in the treated neurons; moreover, reduced levels of phosphorylated receptors were detected in the proximal parts of the axons where Golgi accumulation was also observed. Furthermore, the calibers of these neurites were expanded locally at or near these sites. This dilatation of neurites is also evident when axonal flow is disturbed, a feature typically observed in patients with amyotrophic lateral sclerosis [21]. Thus, these findings support the idea that retrograde axonal transport was disrupted in the -amanitin-treated neurons.

Trafficking problems have been highlighted in some CAG repeat diseases [22], although it is not clear whether axonal traffic is disrupted in cases of SCA 1. Pathologic evidence for axonal transport problems in HD was shown in transgenic mouse models of HD and the brains of human patients with the disease [23,24]. In patients with SCA 6, there is an axonal accumulation of neurofilaments and other materials that fail to be transported [25]. Although the precise mechanisms that cause transport problems are

unclear, it has been proposed that the accumulation of diseased, possibly "sticky" proteins, can physically block transport pathways and move motor proteins away from their normal functions within narrow-caliber axons or dendritic processes [22]. Our results here were obtained without forming protein aggregates, and this suggests that there might be indirect effects of abnormal polyQ proteins for the disruption of axonal transport.

In this study, neurite elongation and maturation were both altered by the -amanitin treatment. In the developing of neuronal process, cytoplasmic dynein generates forces against the actin cytomatrix, which cause the microtubules to move outward [26]. Hafezparast et al. found that disruption of dynein impaired the formation of neuronal processes [27]. These findings support our hypothesis that a minus-end-directed organelle transport system involving dynein might be affected in -amanitin-treated neurons.

It is important to note that the alterations in the distribution of organelles observed in this study occurred when the neurons survived vigorously (6 days after starting the treatment; see Fig. 3A). Treated neurons remained alive at least three more days without any changes in the survival rate compared with the controls. Thus, these changes in organelle distribution may not be directly caused by the death process, but evidently precede it by several days. In conjunction with another report [22], we suggest that perturbations in organelle distribution and perhaps in transport pathways may be early events in the pathology of SCA 1.

Acknowledgement

This study was supported by a Grant-in-Aid for Scientific Research (C) (No. 17590859) from the Ministry of Education, Science, Sports, Culture and Technology, Japan to T. Yamazaki, and was also supported by a grant from the Ministry of Health, Labour and Welfare of Japan to K. Okamoto.

References

[1] Reddy PH, Williams M, Charles V, Garret L, Pike-Buchanan L, Whetsell Jr WO. Behavioral abnormalities and selective neuronal loss in HD transgenic mice expressing mutated full-length HD cDNA. Nat Genet 1998;20:198–202.

[2] Wellington CL, Ellerby LM, Hackam AS, Margolis RL, Trifiro MA, Singaraja R. Caspase cleavage of gene products associated with triplet expansion disorders generates truncated fragments containing the polyglutamine tract. J Biol Chem 1998;273:9158–67.

[3] Hickey MA, Chesselet MF. Apoptosis in Huntington's disease. Prog Neuro-Psychopharmacol Biol Psychiatry 2003;27:255–65.

[4] Kim M, Lee HS, Laforet G, McIntyre C, Martin EJ, Chang P, et al. Mutant huntingtin expression in clonal striatal cells: dissociation of inclusion formation and neuronal survival by caspase inhibition. J Neurosci 1999;19:964–73.

[5] Okazawa H, Rich T, Chang A, Lin X, Waragai M, Kajikawa M, et al. Interaction between mutant ataxin-1 and PQBP-1 affects transcription and cell death. Neuron 2002;34:701–13.

[6] Yamazaki T, Selkoe DJ, Koo EH. Trafficking of cell surface -amyloid precursor protein: retrograde and transcytotic transport in cultured neuron. J Cell Biol 1995;129:431–42.

[7] Brewer GJ, Torricelli JR, Evege EK, Price PJ. Optimized survival of hippocampal neurons in B27-supplemented neurobasal, a new serum-free medium combination. J Neurosci Res 1993;35:567–76.

[8] Herkert M, Shakman O, Schweins E, Becker CM. -Bungarotoxin is a potent inducer of apoptosis in cultured rat neurons by receptor-mediated internalization. Eur J Neurosci 2001;14:821–8.

[9] Du J, Feng L, Zaitsev E, Je HS, Liu XW, Lu B. Regulation of TrkB receptor tyrosine kinase and its internalization by neuronal activity and Ca^{2+} influx. J Cell Biol 2003;163:385–95.

[10] Foud FM, Marshall WD, Farrell PG, Goldberg M, Ruhenstroth-Bauer G. Inhibition by the mushroom toxins -amanitin and phalloidin of hepatoprotein-induced ^{3}H-thymidine incorporation into rat liver DNA and of plasma protein production in hepatocyte cultures. Toxicon 1987;12:1265–71.

[11] Kolodziej PA, Woychik N, Liao SM, Young RA. RNA polymerase II subunit composition, stoichiometry, and phosphorylation. Moll Cell Biol 1990;10: 1915–20.

[12] Nguyen VT, Giannoni F, Dubois MF, Seo SJ, Vigneron M, Kedinger C. In vivo degradation of RNA polymerase II largest subunit triggered by -amanitin. Nucleic Acid Res 1996;24:2924–9.

[13] Bhattacharyya A, Watson FL, Pomeroy SL, Zhang YJ, Stiles CD, Segal RA. High-resolution imaging demonstrates dynein-based vesicular transport of activated Trk receptors. J Neurobiol 2002;51:302–12.

[14] Turmaine M, Raza A, Mahal A, Mangiarini L, Bates GP, Davies SW. Nonapoptotic neurodegeneration in a transgenic mouse model of Huntington's disease. Proc Natl Acad Sci USA 2000;97:8093–7.

[15] Burkhardt JK, Echeverri CJ, Nilsson T, Valee RB. Overexpression of the dynamitin (p50) subunit of the dynactin complex disrupts dynein-dependent maintenance of membrane organelle distribution. J Cell Biol 1997;139:469–84.

[16] Morris RL, Hollenbeck PJ. Axonal transport of mitochondria along microtubules and F-actin in living vertebrate neurons. J Cell Biol 1995;131: 1315–26.

[17] Terasaki M, Reese TS. Characterization of endoplasmic reticulum by co-localization of BiP and dicarbocyanine dyes. J Cell Sci 1992;101: 315–22.

[18] Kreis TE. Role of microtubules in the organization of the Golgi apparatus. Cell Motil Cytoskeleton 1990;15:67–70.

[19] Matteoni R, Kreis TE. Translocation and clustering of endosomes and lysosomes depends on microtubules. J Cell Biol 1987;105:1253–65.

[20] Hirokawa N, Sato-Yoshitake R, Yoshida T, Kawashima T. Brain dynein (MAP1C) localizes on both retrogradely transported membranous organelles in vivo. J Cell Biol 1990;111:1027–37.

[21] Julien JP. Neurofilaments and motor neuron disease. Trends Cell Biol 1997;7:243–9.

[22] Gunawardena S, Goldstein LSB. Polyglutamine disease and transport problems. Arch Neurol 2005;62:46–51.

[23] Difiglia M, Sapp E, Chase KO, Davies SW, Bates GP, Vonsattel JP. Aggregation of huntingtin in neuronal intranuclear inclusions and dystrophic neurites in brain. Science 1997;277:1990–3.

[24] Li H, Li SH, Yu ZX, Li XJ. Huntingtin aggregate-associated axonal degeneration is an early pathological event in Huntington's disease mice. J Neurosci 2001;21:8473–81.

[25] Yang Q, Hashizume Y, Yoshida M, Wang Y, Goto Y, Mitsuma N, et al. Morphological Purkinje cell changes in spinocerebellar ataxia type 6. Acta Neuropathol 2000;100: 371–6.

[26] Gavin RH. Microtubule-microfilament synergy in the cytoskeleton. Int Rev Cytol 1997;173:207–42.

[27] Hafezparast M, Klocke R, Ruhrberg C, Marquardt A, Ahmad-Annuar A, Bowen S, et al. Mutations in dynein link motor neuron degeneration to defects in retrograde transport. Science 2003;300:808–12.

JOURNAL OF CLINICAL MICROBIOLOGY, Jan. 2007, p. 112–120 Vol. 45, No. 1
0095-1137/07/$08.00+0 doi:10.1128/JCM.00718-06

Genetic Diversity of Coxsackievirus A16 Associated with Hand, Foot, and Mouth Disease Epidemics in Japan from 1983 to 2003[▽]

Mitsuaki Hosoya,[1]* Yukihiko Kawasaki,[1] Masatoki Sato,[1] Ken Honzumi,[1] Akio Hayashi,[2] Toyomasa Hiroshima,[2] Hiroaki Ishiko,[2] Kazuo Kato,[3] and Hitoshi Suzuki[1]

Department of Pediatrics, Fukushima Medical University School of Medicine, Fukushima 960-1295,[1] Research and Development Department, Mitsubishi Kagaku Bio-Clinical Laboratories, Inc., Tokyo 174-8555,[2] and Fukushima Institute for Public Health, Fukushima 960-8560,[3] Japan

Received 5 April 2006/Returned for modification 5 July 2006/Accepted 21 October 2006

To clarify the chronologic genetic diversity of coxsackievirus A16 (CV-A16) strains associated with hand, foot, and mouth disease (HFMD) epidemics in a restricted area and their genetic relation with those isolated in other areas, we investigated the genetic diversity of the 129 CV-A16 strains associated with HFMD epidemics in Fukushima, Japan, from 1983 to 2003, and compared their genetic relation to 49 CV-A16 strains isolated in other areas of Japan and in China by using phylogenetic analysis based on the VP4 sequences. Phylogenetic reconstruction of the CV-A16 strains isolated in Fukushima from 1983 to 2003 demonstrated three distinct genetically divergent clusters related to HFMD epidemics that occurred from 1984 to 1994 (including the 1985 and 1991 outbreaks), HFMD epidemics from 1987 to 1998 (including the 1988 and 1998 outbreaks), and HFMD epidemics from 1995 to 2003 (including the 1995 and 2002 outbreaks). CV-A16 strains isolated during each period in Fukushima formed a single cluster with those isolated during essentially the same time period in other areas of Japan and in China. Our results demonstrated that prevalent CV-A16 strains causing HFMD in Fukushima, Japan, genetically changed twice during 21 epidemics, and changes were also observed in the CV-A16 strains causing HFMD epidemics in other areas. We concluded that repeated outbreaks of CV-A16-related HFMD in Japan were caused, in part, by the introduction of genetically changed CV-A16 strains, which might be transmitted overseas.

Coxsackievirus A16 (CV-A16) and human enterovirus 71 (HEV71) are both major etiologic agents of hand, foot, and mouth disease (HFMD). The surveillance data indicate that CV-A16 and HEV71 infections independently cause large outbreaks and then become quiescent for a period of a few years (6).

HEV71-related illness is more severe, with a significantly greater frequency of serious complications and fatality, than illness caused by CV-A16 (2). In 1997, deaths associated with epidemics of HEV71-associated HFMD in Sarawak, Malaysia, followed by outbreaks with high mortality in Taiwan in 1998 and 2000, raised considerable public concern about the virulence of this virus. Since then, several groups have attempted to describe the molecular epidemiology of HEV71 in the Asia-Pacific region and have reported the relationships of HEV71 epidemics with the genetic diversity of HEV71 strains (1, 5, 10). The results indicate that HEV71 strains causing HFMD outbreaks were genetically changed.

On the other hand, the molecular epidemiology of CV-A16 associated with HFMD epidemics has not been fully described (9). In the present study, we evaluated the relationship between the chronologic CV-A16 epidemics in a restricted area, i.e., Fukushima Prefecture, Japan, and the genetic diversity of the CV-A16 strains. We also examined the geographic genetic relationship between the CV-A16 strains isolated in Fukushima and those isolated in other areas of Japan and China, using phylogenetic analyses constructed using the neighbor-joining method on the basis of the VP4 and VP1 sequences.

* Corresponding author. Mailing address: Department of Pediatrics, Fukushima Medical University School of Medicine, Hikarigaoka 1, Fukushima 960-1295, Japan. Phone: 81-24-547-1111. Fax: 81-24-548-6578. E-mail: mhosoya@fmu.ac.jp.

[▽] Published ahead of print on 8 November 2006.

MATERIALS AND METHODS

Virus strains. Pharyngeal swab samples were collected from patients with HFMD in the Fukushima Prefecture for virus surveillance and transferred to the Fukushima Institute for Public Health for virus isolation. HEp-2, Vero, and RD-18 cells were used for the isolation of enteroviruses. Confluent cell cultures were seeded in microplate wells and inoculated with 100 μl of maintenance medium and 50 μl of pharyngeal swab samples. The cell cultures were then incubated at 34°C in 5% CO_2–95% air and observed for 7 days to check for cytopathic effects. A blind passage was performed once if no cytopathic effect was observed by the end of the observation period. Virus isolates were identified by a neutralization test using anti-CV-A16 polyclonal antibodies provided from the National Institute of Infectious Diseases in Japan. A total of 322 CV-A16 strains were isolated and identified from 1983 to 2003. Those isolates were stored at −80°C.

PCR and sequence determination of VP4 gene. Randomly selected isolates (63 of 241 strains) from 1983 to 1999 and all isolates (69 strains) from 2000 to 2003 were used for further genetic analysis. A total of 132 strains were isolated from patients with HFMD. The methods of molecular diagnosis of enteroviruses by nested reverse transcription-PCR (RT-PCR) and phylogeny-based classification using the VP4 sequences are described elsewhere (7). Briefly, viral RNA was directly extracted from 100 μl of the stock virus samples using the Smitest R kit (Genome Science Laboratories) according to the manufacturer's instructions. The RNA was dissolved with 10 μl of RNase-free distilled water containing 40 U of RNase inhibitor (RNasin; Promega) and 50 pmol of a reverse primer, OL68-1 [nucleotides (nt) 1178 to 1197, 5′-GGTAA(C/T)TTCCACCACCA(A/G/C/T)C C-3′]. The positions of the primers for RT-PCR were numbered according to the complete nucleotide sequence of the attenuated poliovirus Sabin 1 strain (11). The RNA was subjected to heat denaturation for 15 s at 100°C, followed by snap-cooling in an ice-water bath. Reaction mixture (10 μl; 200 U of Moloney murine leukemia virus reverse transcriptase [Life Technology], 2.5 mM deoxynucleoside triphosphates, and 40 U of RNasin [Promega]) was added to each RNA sample. cDNA synthesis was performed for 1 h at 37°C. In total, 5 μl of the